Montes Navajas, PM.; Serra, M.; García Gómez, H. (2013). Influence of the irradiation wavelength on the photocatalytic activity of Au-Pt nanoalloys supported on TiO2 for hydrogen generation from water. Catalysis Science and Technology. 3(9):2252-2258. doi:10.1039/c3cy00102d

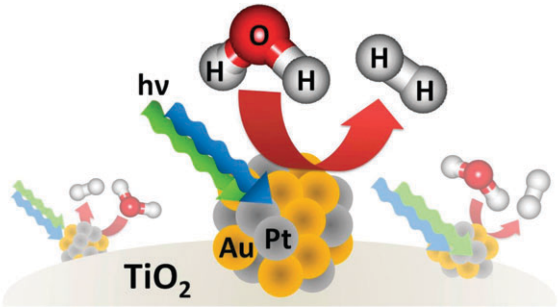

Q2

Influence of the irradiation wavelength on the photocatalytic activity of Au–Pt nanoalloys supported on TiO_2 for hydrogen generation from water

Pedro Montes-Navajas, Marco Serra and Hermenegildo Garcia*

The photocatalytic activity of TiO_2 modified by Au–Pt nanoalloys depends on the presence or absence of methanol as a sacrificial hole quencher and the irradiation light.

Please check this proof carefully. **Our staff will not read it in detail after you have returned it.**

Translation errors between word-processor files and typesetting systems can occur so the whole proof needs to be read. Please pay particular attention to: tabulated material; equations; numerical data; figures and graphics; and references. If you have not already indicated the corresponding author(s) please mark their name(s) with an asterisk. Please e-mail a list of corrections or the PDF with electronic notes attached – do not change the text within the PDF file or send a revised manuscript. Corrections at this stage should be minor and not involve extensive changes. All corrections must be sent at the same time.

Please bear in mind that minor layout improvements, e.g. in line breaking, table widths and graphic placement, are routinely applied to the final version.

Please note that, in the typefaces we use, an italic vee looks like this: v, and a Greek nu looks like this: ν.

We will publish articles on the web as soon as possible after receiving your corrections; **no late corrections will be made.**

Please return your **final** corrections, where possible within **48 hours** of receipt, by e-mail to: catalysis@rsc.org

Queries for the attention of the authors

Journal: **Catalysis Science & Technology**

Paper: **c3cy00102d**

Title: **Influence of the irradiation wavelength on the photocatalytic activity of Au–Pt nanoalloys supported on TiO_2 for hydrogen generation from water**

Editor's queries are marked on your proof like this Q1, Q2, etc. and for your convenience line numbers are indicated like this 5, 10, 15, ...

Please ensure that all queries are answered when returning your proof corrections so that publication of your article is not delayed.

Query reference	Query	Remarks
Q1	For your information: You can cite this article before you receive notification of the page numbers by using the following format: (authors), Catal. Sci. Technol., (year), DOI: 10.1039/c3cy00102d.	
Q2	Please carefully check the spelling of all author names. This is important for the correct indexing and future citation of your article. No late corrections can be made.	
Q3	Please check that telephone number has been displayed correctly.	
Q4	The meaning of the phrase 'renewable energy resources to fossil fuels...' is not clear - please clarify.	
Q5	The sentence beginning ''Compared to conventional...'' has been altered for clarity, please check that the meaning is correct.	
Q6	Please check that the unit 'mol^{-1} L cm' in the sentence beginning 'The possibility that' has been displayed correctly.	
Q7	Ref. 24: Please provide details of the last page number for this article.	

Catalysis
Science & Technology

RSC Publishing

PAPER

Cite this: DOI: 10.1039/c3cy00102d

Influence of the irradiation wavelength on the photocatalytic activity of Au–Pt nanoalloys supported on TiO_2 for hydrogen generation from water

Pedro Montes-Navajas, Marco Serra and Hermenegildo Garcia*

Received 12th February 2013,
Accepted 15th May 2013

DOI: 10.1039/c3cy00102d

www.rsc.org/catalysis

Seven samples of P25 titania containing Au–Pt nanoalloys at constant total metal loading (0.25% wt), very similar particle size (1.5 nm) and different proportions of Pt (0.0, 22.8, 27.8, 35.0, 50.0, 69.0 and 100.0% wt) have been prepared and characterized. Formation of real nanoalloys was supported by the shifts in the binding energy values of Au and Pt $4f_{7/2}$ peaks in XPS. Using 532 nm laser excitation it was observed that the six samples exhibit similar photocatalytic activity for hydrogen generation in the presence of methanol as a sacrificial electron donor. In contrast, in pure water remarkable differences in efficiency for hydrogen generation between the sample containing exclusively Au that was the most active and the others containing Pt were observed. In addition, oxygen evolution was also observed in the absence of methanol under visible light irradiation. Our results illustrate the potential that nanoalloys offer to optimize the photocatalytic activity of TiO_2.

In the context of renewable energy resources to fossil fuels, photocatalytic hydrogen generation by solar light is gaining increasing interest due to the possibility of using hydrogen as a clean transportation fuel.[1–7] In this context, modified TiO_2 is the most widely used photocatalyst.[1,8–13] The main problem to be overcome is the negligible visible light photoresponse of plain TiO_2.[1,5,8,14–24] Among the various possibilities to enhance the visible light photocatalytic activity of TiO_2, one that has attracted considerable interest in recent times is the use of gold nanoparticles (AuNPs) as a light harvester and a photosensitizer for TiO_2.[17,18,21] Compared to conventional metal doping, the use of Au/TiO_2 presents the advantage of reliable preparation procedures, high durability due to the noble metal character of gold and high visible light photocatalytic activity due to the broad absorption originating from the surface plasmon band of AuNPs expanding from 400 to 700 nm. In this Au/TiO_2 photocatalyst, Au may play simultaneously several roles including light absorption and photosensitization of TiO_2 as well as acting as a catalytic centre to yield the photoproducts.[17,18,21]

In this context, it is of interest to assess the relative photocatalytic activity of Au nanoalloys. In particular, in the present manuscript we are concerned with providing comparative data for the photocatalytic activity of TiO_2 P25 modified by Au–Pt nanoalloys. The presence of Pt, with higher catalytic activity than Au in thermal hydrogenation[25] and oxidation,[26] can lead to more efficient photocatalytic activity if the controlling efficiency limiting steps are related to the role of metal NPs as catalysts. On the other hand, the presence of Pt could have a detrimental effect on the photocatalytic activity due to the fact that Pt has no surface plasmon band absorption and the presence of this metal in the nanoalloy could have adverse effects on the light absorption and the electron injection events of the photocatalytic cycle.

In the present work we have compared the photocatalytic activity of Au–Pt nanoalloys under visible, UV or simulated solar light irradiation, both in the presence and absence of methanol as a sacrificial electron donor. For visible light irradiation we used purposely a 532 nm laser excitation (green monochromatic light) to ensure excitation near the Au surface plasmon band absorption maxima (560 nm). In recent related precedents, photocatalytic hydrogen production using Au–Pt/TiO_2 photocatalysts has been studied using UV or solar light excitation and it was concluded that the combination of the Au–Pt nanoalloy (atomic ratio 1 : 1) exhibits the highest photocatalytic activity compared to the samples containing each of the noble metal independently.[27,28] This positive influence exerted by Pt is also in line with previous work using UV light that established the higher activity of Pt over Au for hydrogen generation.[29] Considering these precedents in which apparently

---

Instituto de Tecnologia Quimica (CSIC-UPV), Universidad Politecnica de Valencia, Avenida de los Naranjos s/n, C.P. 46022, Valencia, Spain.
E-mail: hgarcia@qim.upv.es; Fax: +34 963877809; Tel: +34 963877807

the presence of Pt increases the activity of Au under UV light and on the other the fact that Pt has no surface plasmon band that can be used to photosensitize TiO_2, it would be of interest to undertake a study of the photocatalytic activity of Au–Pt alloys under visible light to clarify if, also under these conditions, the presence of Pt increases the photocatalytic activity.

Sample preparation and characterisation

For the present study aimed at determining the relative photocatalytic activity of Au–Pt nanoalloys for visible light hydrogen generation, we have prepared six samples, all of them at the same overall metal loading in which part of the Au has been replaced by an increasing proportion of Pt up to 50%. The list of the samples prepared and the main analytical and spectroscopic data are summarized in Table 1. In these samples the Au–Pt nanoalloys are deposited on commercially available P25 titania, which is a common reference material in the field and exhibits high photocatalytic activity for hydrogen generation under UV light irradiation.

In addition, all the samples were prepared by the well known deposition–precipitation method. This procedure consists of two steps, the first of which is the adsorption of gold species from $AuCl_4^-$ aqueous solutions at controlled pH on the surface of hydroxylated titania (deposition). Subsequently, nucleation and generation of metal NPs is accomplished by Au reduction under various conditions. In our case the samples were treated by a hydrogen flow at 300 °C in order to effect the reduction of Au^{3+} and Pt^{4+} to the corresponding metal state. The overall loading (about 0.25% wt) was selected in the range where previously the highest visible light photocatalytic activity was measured.

Deposition of Au–Pt nanoparticles on P25 titania does not change the Raman spectra or XRD of the solid that correspond basically to that expected for P25 without reflecting the presence of a minor amount of noble metal. The percentage of Au and Pt on the solid was determined by X-ray fluorescence using calibrated standards. Transmission electron microscopy images show the presence of small metal nanoparticles of about 1.5 nm diameter on the titania surface. No notable differences in the particle size distribution were observed for the various samples having different Pt percentage. As we will comment below, this is the average size corresponding to Au–Pt particles, since no independent Au or Pt particles have been observed. Fig. 1 shows selected TEM micrographs of the samples to illustrate the morphology and size of the noble metal nanoparticles.

Table 1 Au–Pt/TiO_2 samples tested in this study and their corresponding total metal loading and Au percentage

Sample	Total metal content[a] (%)	Au (%)
S1	0.247	100.0
S2	0.234	78.2
S3	0.229	72.2
S4	0.255	65.0
S5	0.257	50.0
S6	0.264	31.0
S7	0.233	0.0

[a] Combined weight of Au and Pt metals divided by total sample weight in percentage.

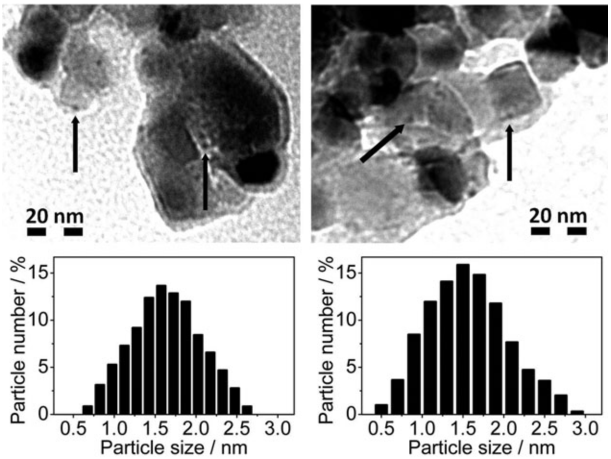

Fig. 1 TEM images of S1 (left) and S4 (right) samples and their corresponding particle size histograms.

Metal alloys can be studied by EDS analysis that allows us to determine the spatial distribution of both metals on the sample. However, since Pt and Au are neighbors in the periodic table, this technique does not allow unfortunately to map out the distribution of both metals. In order to address if our samples contain independent Pt and Au nanoparticles or if real Au/Pt nanoalloys are present we used XPS analysis by determining the binding energies of the components of experimental Au4f7/2 and Pt4f7/2 peaks. XPS probing a depth of about 30 nm of the compressed powdered photocatalyst wafer (thickness of about 800 μm) really gives an indication of the average distribution of Au and Pt atoms in the sample considering that TiO_2 particles are about 50 nm in diameter. The fact that we have observed significant shifts in the binding energy values for the Pt 4f7/2 (76.4 and 75.5 eV for S5 and S6, respectively) as well as for the two components of Au4f7/2 (83.9 and 88.4 eV for S5 with respect to 84.7 and 88.8 eV for S6) strongly suggests the formation of real alloys between Au and Pt at the nanometric scale. Thus, the XPS technique shows that the predominant distribution of Au and Pt forms nanoalloys. Fig. 2 shows the experimental Au 4f7/2 peaks recorded for samples S5 and S6, together with the deconvolution components and the estimated binding energies.

All the samples exhibit the characteristic pink color indicating the presence of AuNPs. In this case, this surface plasmon band should arise from the Au–Pt nanoalloys that are the predominant NPs or from a low proportion of individual Au NPs not detectable by XPS. This color is reflected in UV-Visible optical spectroscopy by the presence of a weak absorption band centered at about 560 nm accompanied by the intense absorption due to P25 band-gap transition. The presence of increasing percentage of Pt is reflected in a gradual decrease in the surface plasmon band intensity but not in noticeable shifts in the λ_{max} position. Fig. 3 presents the corresponding absorption optical

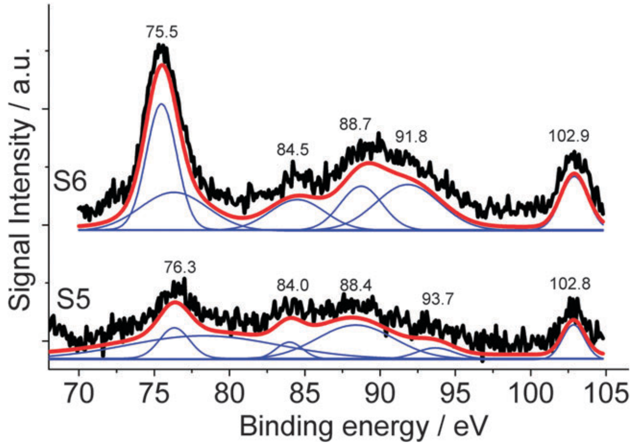

Fig. 2 XPS Au 4f7/2 peak recorded for samples S5 and S6 together with its deconvolution in individual components based on the best fitting of the experimental data.

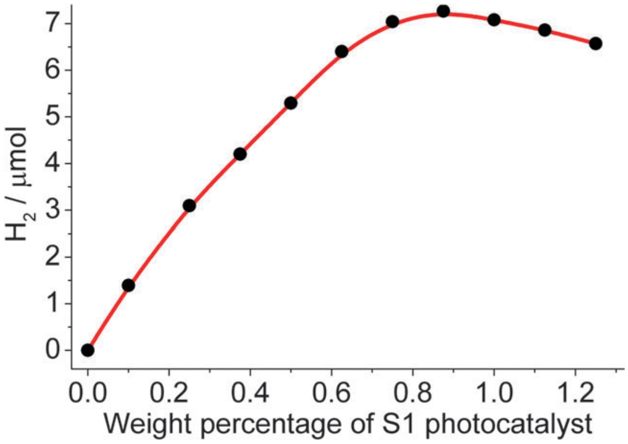

Fig. 4 Influence of the amount of S1 photocatalyst (plotted as weight percentage of S1 in the solution) on the hydrogen evolution after 1000 pulses upon 532 nm laser irradiation.

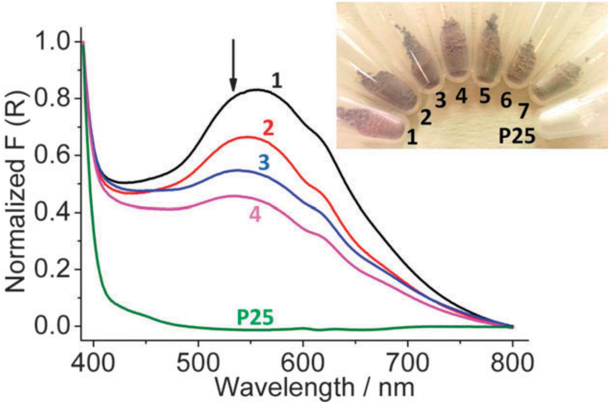

Fig. 3 Diffuse reflectance UV-Vis spectra (plotted as the Kubelka–Munk function of the reflectivity *R*) for some selected samples. The inset shows a photograph of the Au–Pt/TiO_2 samples used in this study.

spectra of some of the Au–Pt/TiO_2 samples to illustrate the changes in the intensity and position of the bands depending on the Pt content. This figure also marks the 532 nm wavelength used for excitation in the present study. Typically the λ_{max} of the surface plasmon band depends on the amount of other parameters and on the size of the nanoparticles. However, as we have commented when discussing Fig. 1 presenting the histogram of particle size distribution, regardless of the Pt content, the size of the nanoparticles is very similar. Therefore, no difference in the position of the surface plasmon band should be expected.

Photocatalytic activity for hydrogen generation under visible light irradiation

To ensure that the photocatalytic hydrogen generation arises from visible light excitation and presumably from excitation of the Au–NP surface plasmon band (λ_{max} on TiO_2 560 nm) all the experiments were carried out with the second harmonic output of a Nd-YAG laser emitting at 532 nm monochromatic light that is close to the maximum absorption for Au NPs. The experiments were carried out by suspending the corresponding photocatalyst in pure water or water containing 20% of methanol as the sacrificial electron donor under continuous stirring.

In preliminary experiments we performed the study of the influence of the amount of photocatalyst present in the system under laser irradiation on the hydrogen generation in order to optimize the evolution of hydrogen. The results are presented in Fig. 4. As it could have been expected, the amount of hydrogen generated increases almost linearly with the amount of Au–TiO_2 photocatalyst up to a certain weight at which further increase even leads to a small decrease in the amount of hydrogen due to the fact that no more photons are absorbed for high weights of the photocatalyst and even light scattering and reflection are gaining importance in opaque dispersions. This optimal amount of photocatalyst was selected for further studies.

Also we initially studied the influence of the laser power on the amount of hydrogen evolved. The data for three different photocatalyst contents are presented in Fig. 5 and show the same trend. No saturation of the hydrogen evolution reaching a plateau at the laser power increases is observed, indicating that, at the weight percentage of catalyst employed, the limiting factor is the number of photons entering into the system. As it can be seen there, the curves of the amount of hydrogen *vs.* laser fluency are not linear but follow a quadratic dependence indicating that the process probably involves the simultaneous absorption of two photons under our irradiation conditions. The possibility that the photocatalytic hydrogen generation under laser irradiation is a bi(multi)photonic process is not totally unreasonable considering that Au-NPs may have a very Q6 large extinction coefficient (estimated to be $\sim 10^9$ mol^{-1} L cm) for 20 nm nanoparticles and the large photon fluency of the laser pulse. Although the exact power may vary from one experiment to other, the range of laser power was in the 300 mW region to ensure high ability for hydrogen generation. As it can be seen in Fig. 5, under the experimental conditions used in

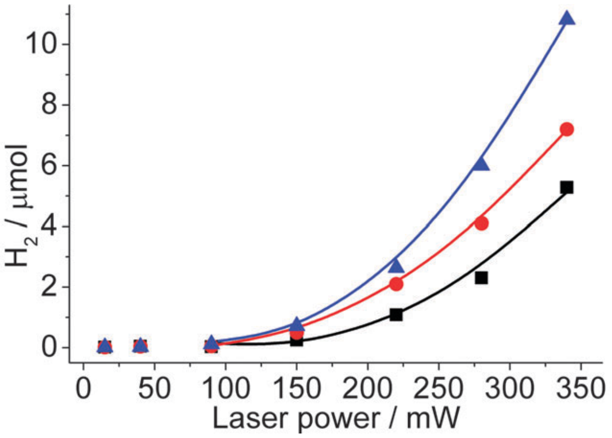

Fig. 5 Influence of laser power on the hydrogen evolution upon 532 nm laser irradiation of 0.1 (■), 0.25 (●) or 0.5 (▲) wt% of S1 catalyst in a methanol–water solution (20 : 80). The continuous line corresponds to the best fitting of the experimental points to a quadratic equation.

this work (0.8 wt% and 300 mW), the limiting parameter for hydrogen evolution is the light intensity, *i.e.* higher light fluencies will lead to higher H_2 evolution.

Contrasting results depending on the presence or absence of methanol were obtained. The results are shown in Fig. 6 and 7. As expected in view of the well established influence of methanol, the amount of hydrogen observed in the photolysis when this sacrificial agent was present was considerably larger than in its absence. Preliminary blank controls using TiO_2 subjected to the same experimental protocol as that followed for the preparation of the S1 sample show some hydrogen evolution (see Fig. 6) but was nine times lower than that measured for the S1 sample. This weak photocatalytic activity of TiO_2 at 532 nm can be due to Raman laser scattering of the beam crossing the suspension that has a weak component at 415 nm. Importantly, no appreciable differences in the photocatalytic activity of the samples tested were observed in the presence of methanol.

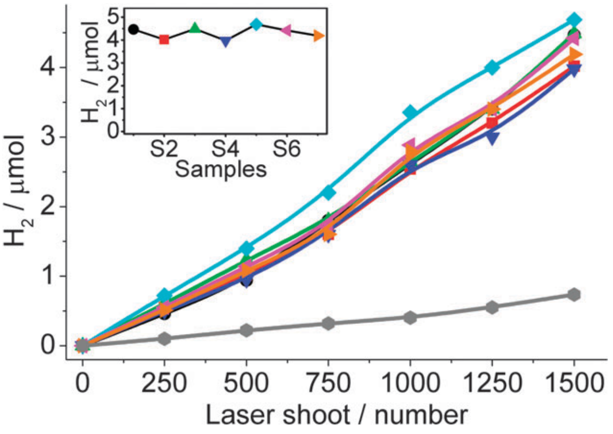

Fig. 6 Temporal hydrogen evolution upon 532 nm laser irradiation of 1 mL of a methanol aqueous solution (20 wt%) containing 5 mg of photocatalyst. The inset shows the efficiency of H_2 generation in methanol–water for the photocatalysts tested for 1500 pulses. Color and symbol code: S1 (●), S2 (■), S3 (▲), S4 (▼), S5 (◆), S6 (◀), S7 (▶) and P25 (⬢).

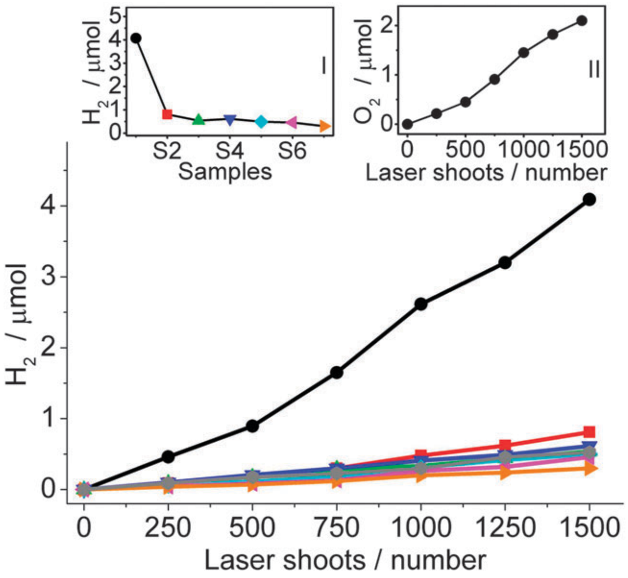

Fig. 7 Temporal hydrogen evolution upon 532 nm laser irradiation of 1 mL of pure water containing 5 mg of photocatalyst. Inset I shows the relative efficiency for H_2 generation in water of the photocatalysts tested for 1500 pulses. Inset II shows, on the other hand, the oxygen evolution corresponding to S1 in the same experiment as the one in which H_2 was measured. Color and symbol code: S1 (●), S2 (■), S3 (▲), S4 (▼), S5 (◆), S6 (◀), S7 (▶) and P25 (⬢).

Thus, the increasing percentage of Pt up to 50% in the nanoalloy does not play any influence on the efficiency.

In contrast, in the absence of methanol, although the volume of hydrogen evolved was significantly lower than when methanol is present, remarkable differences were observed depending on the presence of Pt. Preliminary experiments using the parent TiO_2 sample subjected to the same treatments as those followed to prepare S1 show that the hydrogen generation under these conditions was negligible compared to the S1 sample. Concerning the influence of Pt, the most efficient photocatalyst was the one in which no Pt was present (Au/TiO_2), the presence of Pt producing a significant decrease in the photocatalytic activity (see Fig. 7). This negative effect is observed even at the lowest Au–Pt atomic ratio tested. In fact, as inset in Fig. 7 shows, the activity of all the samples containing some Pt was relatively constant.

Considering the well known catalytic activity of Pt as a hydrogen evolving center, these data seem to suggest that the rate determining step is not hydrogen evolution but other elementary processes taking place in the photocatalysis such as light absorption and electron injection of hot electrons from Au to the conduction band of the semiconductor or hole (h^+) quenching.

In this context, it is interesting to comment that in the photolysis of neat water, evolution of oxygen for the Au/TiO_2 photocatalyst was observed in the expected stoichiometrical amount (see inset II in Fig. 7). Although experimental evidence of interfaced electron injection from excited AuNP to the conduction band of TiO_2 is still missing, a mechanistic proposal based on charge separation with electrons located on the

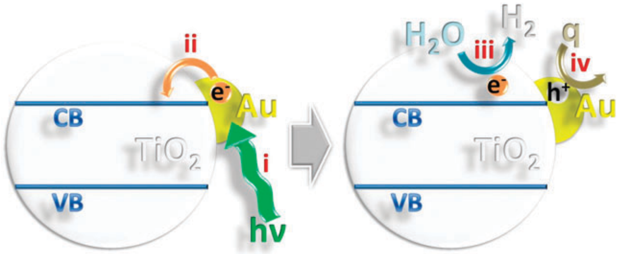

Scheme 1 Proposed mechanism for visible light photocatalytic activity of Au/TiO_2. CB: conduction band, VB: valence band, i: light absorption, ii: electron injection, iii: water reduction, iv: hole quenching.

semiconductor and the positive hole on the AuNP has been suggested.[21] Scheme 1 illustrates the proposed mechanism for hydrogen generation upon visible light irradiation of the Au/TiO_2 photocatalyst. The key point is whether or not the oxidation potential of this h^+ site on AuNPs is still sufficiently high to effect water oxidation (E^o_{ox} = 1.26 V). Obviously, in the case that methanol is present, the formation of oxygen was not observed.

Photocatalytic activity of Au–Pt/TiO_2 under UV light or simulated sun light

As commented earlier, the current challenge in photocatalytic hydrogen generation from solar light is to develop an efficient material under solar light illumination. While sun light contains about 48% of energy in the visible region and only about 4% in the UV zone, it is frequently observed that the minor percentage of UV light is responsible for a large proportion of the photocatalytic activity, particularly for titania photocatalysts. Therefore, we were also interested in determining the relative activity of Au–Pt/TiO_2 materials under UV light and simulated solar light. As we have already commented, precedents in the literature have already established that in the presence of UV radiations, Au–Pt nanoalloys are more efficient to enhance the photocatalytic activity of TiO_2 than each of the noble metals independently.[27,28] However, these studies were carried out at higher noble metal loadings (1 and 2% wt compared to the 0.25% reported here) and also for only one Au–Pt ratio (1 : 1). For this reason, our data have the interest to provide further information to establish the optimal proportion between Pt and Au. In addition, the likely differences in the photocatalytic activities of the Au–Pt/TiO_2 in the UV and in the visible range make difficult to predict the exact ranking of efficiencies under simulated solar light.

In accordance with the previous report of Dal Santo and coworkers,[28] under monochromatic 300 nm irradiation using methanol as the sacrificial electron donor, the less efficient sample was material S1 containing pure AuNPs. The efficiency under monochromatic UV irradiation increases with the presence and proportion of Pt, the most efficient ones being those having the largest Pt content (photocatalysts S6 and S7). Fig. 8 presents the hydrogen evolution *vs.* time under 300 nm irradiation. Worth noting is the fact that the ranking of activity under UV light is different to that previously measured under monochromatic visible light and in general agreement with the precedents shows the higher photoactivity of Pt containing photocatalysts *vs.* those containing Au.

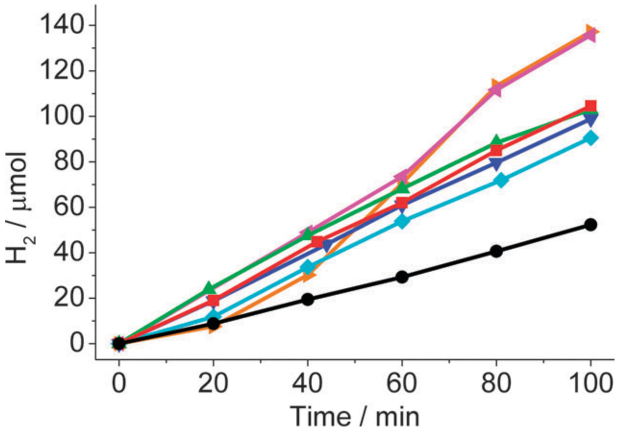

Fig. 8 Temporal hydrogen evolution upon monochromatic 300 nm irradiation. Color and symbol code: S1 (●), S2 (🟥), S3 (▲), S4 (▼), S5 (◆), S6 (◀) and S7 (▶).

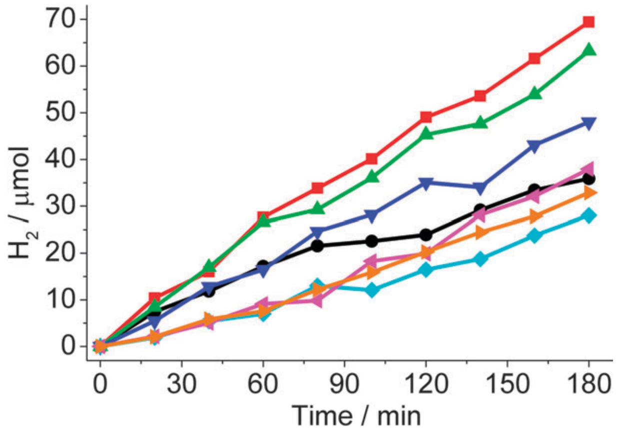

Fig. 9 Temporal hydrogen evolution upon solar simulated irradiation. Color and symbol code: S1 (●), S2 (🟥), S3 (▲), S4 (▼), S5 (◆), S6 (◀) and S7 (▶).

In view of this contrasting behavior depending on the irradiation wavelength, either 532 or 300 nm, it is of interest to determine the actual efficiency upon irradiation with polychromatic simulated sun light. The results of hydrogen generation in a mixture of water–methanol (80 : 20 wt%) using a solar simulator are shown in Fig. 9. Not surprisingly considering the different efficiency ranking between visible light (no influence of the proportion of Pt when methanol is present) and UV light (samples S6 and S7 having the highest Pt proportion are the most efficient), the results using simulated sun light are also different, the presence of a small proportion of Pt in the Au–Pt nanoalloys (samples S2 and S3) appearing now as the most efficient photocatalysts.

Role of Pt in Au–Pt/TiO_2

After having performed the previous experiments using visible, UV or polychromatic light as well as performing the experiments in the presence or absence of the sacrificial electron donor (methanol) the following general trends concerning the influence of Pt content on the nanoalloys can be deduced based on a rationalization that takes into account which is the light harvesting moiety and the influence of a fast hydrogen evolution. When UV light is used for excitation, photons should be mainly absorbed by TiO_2 and then the presence of a large percentage of Pt in the nanoalloy is beneficial because it accelerates hydrogen evolution (see Fig. 8). In contrast, when using exclusively visible light, photons should be absorbed by AuNPs and, in this case, the presence of Pt is detrimental when hydrogen evolution is not the controlling step (Fig. 7) or does not play any role when faster hydrogen evolution is promoted by some Pt in the cluster (Fig. 6). Under sunlight illumination that has a combination of UV and visible light, the situation is a balance between visible light absorption disfavored by the presence of Pt and faster hydrogen evolution promoted by Pt reaching a compromise with an optimal Pt content in the nanoalloy (Fig. 9).

Conclusions

By preparing a set of samples with the same overall metal loading (about 0.25 wt%) but varying the proportion of Pt, we have observed that in the absence of methanol as a sacrificial electron donor, a remarkable decrease in the photocatalytic activity at 532 nm is observed when Pt is present in the nanoparticles. In contrast, when methanol as a h^+ quencher is added to water, similar photocatalytic activity under 532 nm irradiation is observed for all the Au–Pt nanoalloys supported on P25. The order is different when the photocatalysts are excited at 300 nm in the presence of methanol, whereby the photocatalyst having the highest Pt content appears to be the most efficient one. When a solar simulator is used as an excitation source (continuous emission from 380 to 1000 nm) then, an optimal percentage of Pt in the nanoalloy is observed. These results on one hand confirm the controversial visible light photocatalytic activity of Au/TiO_2 and on the other hand show the difference in the photocatalytic activity ranking depending on the excitation wavelength (monochromatic 532 nm or polychromatic UV-Vis irradiation). Controls comparing the photocatalytic activity of a TiO_2 sample subjected to the same treatments used to prepare Au/TiO_2 show in fact some hydrogen evolution with the 532 nm laser but with considerably (at least nine times) lower efficiency than when Au was present. The reason for this contrasting behavior appears to be direct excitation on the TiO_2 semiconductor or photosensitization by the metal nanoparticles surface plasmon band. Further studies are still necessary to fully delineate the differences between UV and visible light irradiation in these systems and to understand and rationalize the origin of these differences. Our results show the potential of nanoalloys, allowing multiple metal combinations, to optimize the photocatalytic activity of TiO_2.

Experimental section

Pre-treated commercial titania P25 (calcination at 450 °C for 3 h) was added to 100 mL basic aqueous solutions (pH 10 adjusted with 0.2 M NaOH) containing 0.25 wt% of $HAuCl_4 \cdot 3H_2O$ and $H_2PtCl_6 \cdot 6H_2O$ in different molar proportions. The resulting suspensions were stirred for 20 h and the solid was filtered, washed with MilliQ water (1 L per gram of catalyst) and dried overnight at room temperature under vacuum. Au–Pt supported nanoalloys were finally obtained by sample reduction using a H_2 flow (80 mL min^{-1}) in an oven at 300 K for 5 h.

X-ray photoelectron spectroscopy (XPS) measurements were performed on a SPECS spectrometer with a Phoibos MCD-9 detector and using a non-monochromatic Al Kα (1486.6 eV) X-ray source. Spectra were recorded using an analyzer pass energy of 50 V, an X-ray power of 50 W and under an operating pressure of 10^{-9} mbar. Spectrum treatment has been performed using the CASA software. Binding energies were referenced to C 1s at 284.5 eV.

Visible light hydrogen generation using monochromatic 532 nm excitation was performed with the second harmonic of a Nd-YAG laser working with a laser power fixed to about 300 mW per pulse and the time width was 7 ns at fwhp. Aqueous or methanol : water (20 : 80 wt%) suspensions of the different photocatalysts (2 mL total volume with 0.8 wt% of the solid under optimized conditions, see Fig. 3) were placed in a capped quartz cuvette and purged with Ar for 10 min. The hydrogen produced by each photocatalyst after irradiating with different number of laser pulses was determined by injecting 50 μL of the head into a GC coupled with a TCD detector using N_2 as calibration standard.

Photocatalytic tests for hydrogen production using monochromatic 300 nm irradiation from a Hamamatsu LC8 source were carried out placing purged (2 psi of Ar for 15 min) and sonicated (15 min) suspension of the catalyst (25 mL, 0.5 g L^{-1}) in a closed reactor with an irradiation window of 12.56 cm^2 provided with temperature and pressure controllers. The evolution of hydrogen during time of irradiation was measured.

Photoreaction using a solar simulator was performed using a Thermo Oriel 1000 W with an irradiation spot of 100 cm^2. The light of the solar simulator was filtered through an Air Mass 1.5 filter, which contains approximately 5% of UV radiation. Hydrogen generation was analyzed *vs.* time of irradiation.

The amount of hydrogen generated in all the experiments was determined by sampling 50 μL of the gas contained in the headspace of the sample containers with a gas syringe and injected into a calibrated gas chromatograph using nitrogen for quantification.

Acknowledgements

Financial support from the Spanish Ministry of Economy and Competitiveness (CTQ2012-31325) is gratefully acknowledged. P. Montes-Navajas also thanks the Universidad Politecnica de Valencia for a postdoctoral contract for excellence (CEI-01-11, 20090796).

Notes and references

1 G. Centi and S. Perathoner, Towards Solar Fuels from Water and CO_2, *ChemSusChem*, 2010, **3**(2), 195–208.
2 G. W. Crabtree, M. S. Dresselhaus and M. V. Buchanan, The hydrogen economy, *Phys. Today*, 2004, **57**(12), 39–44.

3 S. Dunn, Hydrogen futures: Toward a sustainable energy system, *Int. J. Hydrogen Energy*, 2002, **27**(3), 235–264.

4 D. Gust, T. A. Moore and A. L. Moore, Solar Fuels *via* Artificial Photosynthesis, *Acc. Chem. Res.*, 2009, **42**(12), 1890–1898.

5 L. Hammarström and S. Hammes-Schiffer, Artificial Photosynthesis and Solar Fuels, *Acc. Chem. Res.*, 2009, **42**(12), 1859–1860.

6 A. Haryanto, S. Fernando, N. Murali and S. Adhikari, Current status of hydrogen production techniques by steam reforming of ethanol: a review, *Energy Fuels*, 2005, **19**(5), 2098–2106.

7 N. S. Lewis and D. G. Nocera, Powering the planet: chemical challenges in solar energy utilization, *Proc. Natl. Acad. Sci. U. S. A.*, 2006, **103**(43), 15729–15735.

8 V. Balzani, A. Credi and M. Venturi, Photochemical conversion of solar energy, *ChemSusChem*, 2008, **1**(1–2), 26–58.

9 A. J. Bard and M. A. Fox, Artificial photosynthesis – solar splitting of water to hydrogen and oxygen, *Acc. Chem. Res.*, 1995, **28**(3), 141–145.

10 C. C. Chen, P. X. Lei, H. W. Ji, W. H. Ma, J. C. Zhao, H. Hidaka and N. Serpone, Photocatalysis by titanium dioxide and polyoxometalate/TiO_2 cocatalysts. Intermediates and mechanistic study, *Environ. Sci. Technol.*, 2004, **38**(1), 329–337.

11 X. Chen and S. S. Mao, Titanium dioxide nanomaterials: synthesis, properties, modifications, and applications, *Chem. Rev.*, 2007, **107**(7), 2891–2959.

12 A. Fujishima, X. Zhang and D. A. Tryk, TiO_2 photocatalysis and related surface phenomena, *Surf. Sci. Rep.*, 2008, **63**, 515–582.

13 K. Maeda and K. Domen, Photocatalytic Water Splitting: Recent Progress and Future Challenges, *J. Phys. Chem. Lett.*, 2006, **1**(18), 2655–2661.

14 C. Burda, Y. B. Lou, X. B. Chen, A. C. S. Samia, J. Stout and J. L. Gole, Enhanced nitrogen doping in TiO_2 nanoparticles, *Nano Lett.*, 2003, **3**(8), 1049–1051.

15 J. M. Herrmann, Heterogeneous photocatalysis: fundamentals and applications to the removal of various types of aqueous pollutants, *Catal. Today*, 1999, **53**(1), 115–129.

16 M. I. Litter and J. A. Navio, Photocatalytic properties of iron-doped titania semiconductors, *J. Photochem. Photobiol., A*, 1996, **98**(3), 171–181.

17 A. Primo, A. Corma and H. Garcia, Titania supported gold nanoparticles as photocatalyst, *Phys. Chem. Chem. Phys.*, 2011, **13**(3), 886–910.

18 A. Primo, T. Marino, A. Corma, R. Molinari and H. Garcia, Efficient Visible-Light Photocatalytic Water Splitting by Minute Amounts of Gold Supported on Nanoparticulate CeO_2 Obtained by a Biopolymer Templating Method, *J. Am. Chem. Soc.*, 2011, **133**(18), 6930–6933.

19 S. Sakthivel, M. Janczarek and H. Kisch, Visible light activity and photoelectrochemical properties of nitrogen-doped TiO_2, *J. Phys. Chem. B*, 2004, **108**(50), 19384–19387.

20 N. Serpone, D. Lawless and R. Terzian, Solar fuels: status and perspectives, *Solar Energy*, 1992, **49**(4), 221–234.

21 C. G. Silva, R. Juarez, T. Marino, R. Molinari and H. Garcia, Influence of Excitation Wavelength (UV or Visible Light) on the Photocatalytic Activity of Titania Containing Gold Nanoparticles for the Generation of Hydrogen or Oxygen from Water, *J. Am. Chem. Soc.*, 2011, **133**(3), 595–602.

22 H. J. Yan, J. H. Yang, G. J. Ma, G. P. Wu, X. Zong, Z. B. Lei, J. Y. Shi and C. Li, Visible-light-driven hydrogen production with extremely high quantum efficiency on Pt–PdS/CdS photocatalyst, *J. Catal.*, 2009, **266**(2), 165–168.

23 J. C. Yu, W. K. Ho, J. G. Yu, H. Yip, P. K. Wong and J. C. Zhao, Efficient visible-light-induced photocatalytic disinfection on sulfur-doped nanocrystalline titania, *Environ. Sci. Technol.*, 2005, **39**(4), 1175–1179.

24 X. Zong, H. J. Yan, G. P. Wu, G. J. Ma, F. Y. Wen, L. Wang and C. Li, Enhancement of photocatalytic H_2 evolution on CdS by loading MOS_2 as cocatalyst under visible light irradiation, *J. Am. Chem. Soc.*, 2008, **130**(23), 7176–+. Q7

25 A. Corma, P. Serna, P. Concepcion and J. J. Calvino, Transforming nonselective into chemoselective metal catalysts for the hydrogenation of substituted nitroaromatics, *J. Am. Chem. Soc.*, 2008, **130**(27), 8748–8753.

26 T. Mallat and A. Baiker, Oxidation of alcohols with molecular oxygen on solid catalysts, *Chem. Rev.*, 2004, **104**(6), 3037–3058.

27 A. Gallo, M. Marelli, R. Psaro, V. Gombac, T. Montini, P. Fornasiero, R. Pievo and V. Dal Santo, Bimetallic Au–Pt/TiO_2 photocatalysts active under UV-A and simulated sunlight for H_2 production from ethanol, *Green Chem.*, 2012, **14**(2), 330–333.

28 A. Gallo, T. Montini, M. Marelli, A. Minguzzi, V. Gombac, R. Psaro, P. Fornasiero and V. Dal Santo, H_2 Production by Renewables Photoreforming on Pt–Au/TiO_2 Catalysts Activated by Reduction, *ChemSusChem*, 2012, **5**(9), 1800–1811.

29 G. R. Bamwenda, S. Tsubota, T. Kobayashi and M. Haruta, Photoinduced hydrogen-production from an aqueous-solution of ethylene-glycol over ultrafine gold supported on TiO_2, *J. Photochem. Photobiol., A*, 1994, **77**(1), 59–67.